

Space Debris Capturing Tether-Net System Simplified as a 2-D Problem

Feng Liu Prithvi Poddar
UB id: 50361864 UB id: 50539221

1 Introduction

The increasing amount of space debris in Low Earth Orbit (LEO) poses a significant threat to the operational safety of current and future space missions [1], creating an urgent need for reliable and efficient debris removal solutions. Active Debris Removal (ADR) is one of the solutions that show the potential to mitigate the issue [2], and among which, tether-net systems prove to be effective for the capture of uncooperative debris with their high flexibility and long capturing range [3]. In a passive tether-net system, a net is docked and connected to a satellite through a main tether and is launched toward the space debris when the satellite reaches a pre-defined location. The launched net approaches and wraps around the target to make the capture, and then the satellite drags the target to a graveyard orbit for disposal. Multiple researchers illustrated that transforming this passive system to an active robotic tether-net system is a promising method to increase further the robustness and reliability of space debris capture missions [4–9]. On such systems, multiple Maneuverable Units (MUs) are attached to the edges or corners of the net to transport it to the target, enabling increased effective deployment distance compared to purely passive designs. The following figure represents the overall setup of a tether-net system for capturing space debris:

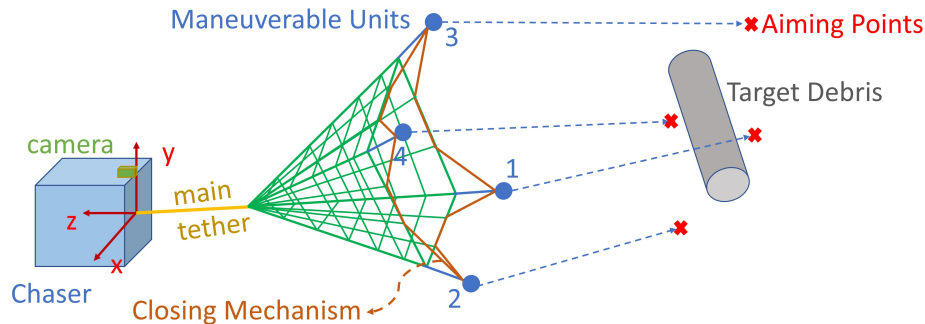


Figure 1: Diagram of the Robotic Tether-Net System

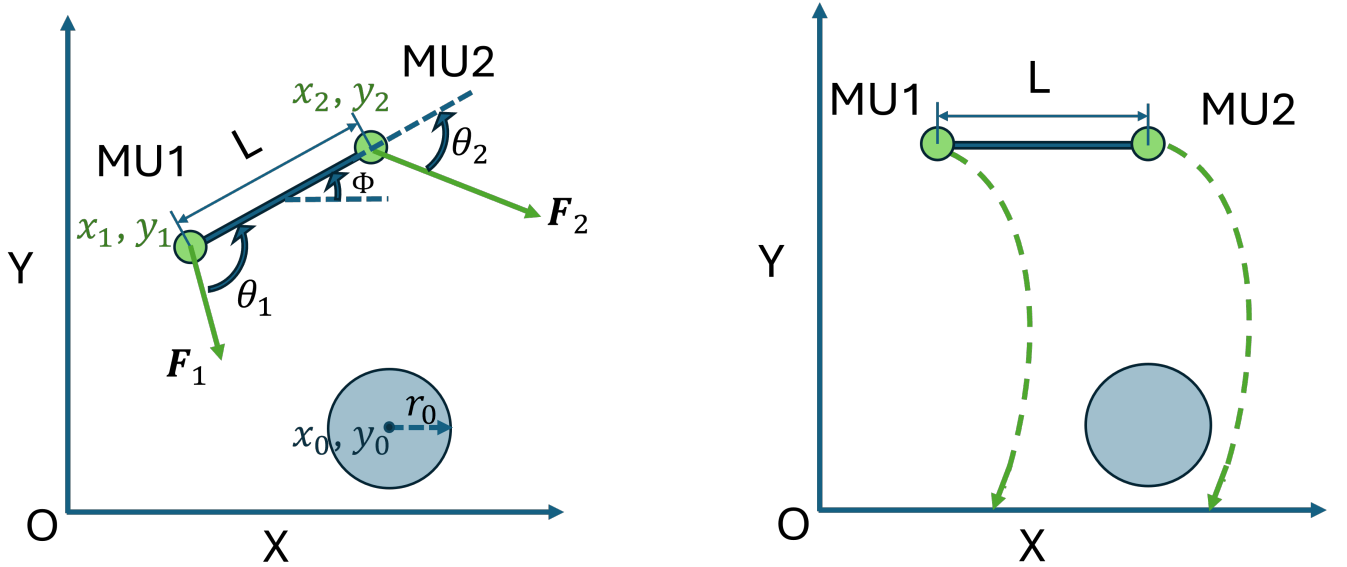
Figure 1 shows the example of a robotic tether-net system. Here chaser refers to the satellite that the net and the MUs were initially attached to. Compared to the target debris, the mass of the MUs and the net are much smaller, so we assume that the dynamics of the target are not affected by the contact of the net nor the MUs.

In this project, we simplify the tether-net system into a 2-D problem with two MUs that can move in the XY plane using thrust vectoring. Similarly, we also consider the debris to be a 2-D circular object and the net must be guided towards the debris. We present two case-studies in the further sections. The first case study (conducted by Prithvi) assumes the tether-net to be a rigid massless rod that connects the two MUs and MUs are assumed to have a constant mass throughout the mission duration. The second case study (conducted by Feng) assumes the tether-net to be flexible while also considering the MU's masses to change over time depending on the amount of thrust they generate.

2 Case Study 1: Fixed Mass MUs With a Rigid Connection Between Them (Conducted by Prithvi Poddar)

In the first case study, we consider the masses of the thrusters/maneuverable units (MUs) to be constant, and the connection between them is a rigid massless rod.

Fig.2a shows the free body diagram of the tether-net system reduced to a 2-D problem. The MUs are controlled by thrust vectoring where $\mathbf{F}_1(t)$ and $\mathbf{F}_2(t)$ are the thrust forces generated by MU1 and MU2 respectively. $\theta_1(t)$ and $\theta_2(t)$ are the thrust vectoring angles of the MUs, measured w.r.t the rod connecting the MUs. The MUs have same masses m and their positions in a global coordinate frame are defined by their x-y coordinates (x_1, y_1) and (x_2, y_2) . The debris is considered to be a circular convex hull located at (x_o, y_o) with a radius of r_o . The length of the rigid rod connecting the two MUs is L and the angle that the rod makes with the X-axis is $\phi(t)$.



(a) Free body diagram of the tether-net system as a 2D problem. The MUs are shown in green while the rigid connection between them is shown in blue. The debris to be captured is represented as a blue circular convex hull.

(b) Diagrammatic representation of the mission objective. The thrusters must fire in a way that drives the tether-net towards the debris to be captured, such that the MUs do not collide with the convex hull of the debris.

Figure 2

Given this information, we can define the system dynamics of the tether-net and the objective function. The mission objective is to guide the center of the net to the debris as quickly as possible and thus we will work with the system dynamics of the center of mass of the tether-net. Since we considered the masses of the MUs to be constant, we can assume that the fuel consumption of the thrusters is insignificant for the mission duration. Thus we do not enforce any constraints on the magnitude of thrust generated during the mission. In the second case study, Sec.3 conducted by my teammate Feng, we relax this assumption and add additional constraints on the thrust magnitudes. The next section derives the system dynamics.

2.1 System Dynamics

Let the center of mass of the tether-net be located at $\mathbf{X}_{\text{com}}(t) = [x_{\text{com}}(t), y_{\text{com}}(t)]^T$. Then the positions of the MUs can be computed as

$$\begin{bmatrix} x_1(t) \\ y_1(t) \end{bmatrix} = \mathbf{X}_{\text{com}}(t) - \frac{L}{2} \begin{bmatrix} \cos(\phi(t)) \\ \sin(\phi(t)) \end{bmatrix}$$

$$\begin{bmatrix} x_2 \\ y_2 \end{bmatrix} = \mathbf{X}_{\text{com}}(t) + \frac{L}{2} \begin{bmatrix} \cos(\phi(t)) \\ \sin(\phi(t)) \end{bmatrix}$$

and the relative positions of the MUs w.r.t the center of mass can be written as

$$\begin{aligned} \mathbf{X}_{1\text{rel}}(t) &= -\frac{L}{2} \begin{bmatrix} \cos(\phi(t)) \\ \sin(\phi(t)) \end{bmatrix} \\ \mathbf{X}_{2\text{rel}}(t) &= \frac{L}{2} \begin{bmatrix} \cos(\phi(t)) \\ \sin(\phi(t)) \end{bmatrix} \end{aligned}$$

Let $F_{1x}(t), F_{1y}(t)$ be the X and Y components of thrust force $\mathbf{F}_1(t)$ acting on MU1 and $F_{2x}(t), F_{2y}(t)$ be the X and Y components of the thrust force $\mathbf{F}_2(t)$ acting on MU2. Then we can write:

$$\begin{aligned} F_{1x}(t) &= \mathbf{F}_1(t) \cos(\theta_1(t) - \phi(t)) \\ F_{1y}(t) &= -\mathbf{F}_1(t) \sin(\theta_1(t) - \phi(t)) \\ F_{2x}(t) &= \mathbf{F}_2(t) \cos(\theta_2(t) - \phi(t)) \\ F_{2y}(t) &= -\mathbf{F}_2(t) \sin(\theta_2(t) - \phi(t)) \end{aligned}$$

With the force components and the relative positions of the thrusters, we can derive the net torque on the tether-net. Torque τ_1 due to the forces on MU1 is

$$\begin{aligned} \tau_1 &= \mathbf{X}_{1\text{rel}}(t) \times \mathbf{F}_1(t) \\ &= \det \begin{bmatrix} \hat{i} & \hat{j} & \hat{j} \\ -\frac{L}{2} \cos(\phi(t)) & -\frac{L}{2} \sin(\phi(t)) & 0 \\ F_{1x}(t) & F_{1y}(t) & 0 \end{bmatrix} \\ \tau_1 &= \left(-\frac{L}{2} \cos(\phi(t)) \right) F_{1y}(t) - \left(-\frac{L}{2} \sin(\phi(t)) \right) F_{1x}(t) \end{aligned}$$

The torque due to the thrust acting on MU2 can be written as

$$\tau_2 = \left(\frac{L}{2} \cos(\phi(t)) \right) F_{2y}(t) - \left(\frac{L}{2} \sin(\phi(t)) \right) F_{2x}(t)$$

Thus the net torque on the tether-net is

$$\begin{aligned} \tau(t) &= \tau_1 + \tau_2 \\ \tau(t) &= \frac{L}{2} [(F_{2y}(t) - F_{1y}(t)) \cos(\phi(t)) - (F_{2x}(t) - F_{1x}(t)) \sin(\phi(t))] \end{aligned}$$

The moment of inertia of the system is

$$I = \frac{mL^2}{2}$$

Finally, using all the information provided above, we can derive the system dynamics of the center of mass as follows:

$$\ddot{x}_{\text{com}}(t) = \frac{F_{1x}(t) + F_{2x}(t)}{2m} \quad (1)$$

$$\ddot{y}_{\text{com}}(t) = \frac{F_{1y}(t) + F_{2y}(t)}{2m} \quad (2)$$

$$\ddot{\phi}(t) = \frac{2}{mL} [(F_{2y}(t) - F_{1y}(t)) \cos(\phi(t)) - (F_{2x}(t) - F_{1x}(t)) \sin(\phi(t))] \quad (3)$$

and the state variables are $\mathbf{X} = [x_{\text{com}}(t), \dot{x}_{\text{com}}(t), y_{\text{com}}(t), \dot{y}_{\text{com}}(t), \phi(t), \dot{\phi}(t)]^T$

2.2 Objective Function

The objective of this case study, as mentioned earlier, is to guide the center of mass of the tether-net to the center of the convex hull of the debris, in the shortest time possible. For this, we define the cost function as

$$\min J = \gamma_1 \sqrt{(x_{com}(t_f) - x_o)^2 + (y_{com}(t_f) - y_o)^2} + \gamma_2 t_f \quad (4)$$

where γ_1 and γ_2 are scalar weighting factors for the 2 components of the objective function. This objective function will drive the center of mass of the tether-net to the center of the debris while also minimizing the total time it takes to reach the debris.

2.3 Constraints

The only constraint we have is that the MUs should not collide with the debris, or in other words, none of the MUs should not enter the convex hull of the debris. This can be ensured by the following inequality constraints:

$$(x_1(t) - x_o)^2 + (y_1(t) - y_o)^2 \geq r_o^2 \quad (5)$$

$$(x_2(t) - x_o)^2 + (y_2(t) - y_o)^2 \geq r_o^2 \quad (6)$$

Additional constraints on the control variables are:

$$0 \leq \mathbf{F}_1(t), \mathbf{F}_2(t) \leq 5\mathbf{N} \quad (7)$$

$$0 \leq \theta_1(t), \theta_2(t) \leq 2\pi \quad (8)$$

2.4 Solving the Optimal Control Problem

Given the system dynamics, the objective function, and the constraints, we use the direct collocation method to solve for the optimal control input. But it can be noticed that this problem is a free final time problem as the final time t_f is free. In order to use direct collocation, we first convert this problem into a fixed final time problem.

Consider a free final time problem with the system dynamics

$$\dot{X} = f(X, u, t)$$

and the cost function

$$\min J = \Phi(X(t_f), t_f) + \int_0^{t_f} L(X, u, t) dt$$

The problem is converted into a fixed final-time problem by introducing a secondary non-dimensional time variable $\zeta = \frac{t}{t_f}$ such that $t = 0 \rightarrow \zeta = 0$ and $t = t_f \rightarrow \zeta = 1$. Thus $\zeta \in [0, 1]$. Then we can write

$$\frac{d}{dt} = \frac{d}{d(\zeta t_f)} = \frac{1}{t_f} \frac{d}{d\zeta} \implies \frac{dX}{d\zeta} = t_f \frac{dX}{dt} = t_f f(X, u, \zeta)$$

Using this, the new augmented system dynamics can be written as

$$\begin{aligned} \dot{X} &= t_f f(X, u, \zeta) \\ \dot{z} &= 0, \text{ such that } z(0) = t_f \text{ and } z(1) = t_f \end{aligned}$$

and the cost function can be written as

$$\min J = \Phi(X(1), t_f) + t_f \int_0^1 L(X, u, \zeta) d\zeta$$

2.5 Results

We finally, test the direction collocation method for three different sets of initial conditions. In all the test cases, the debris is placed at the global origin such that $(x_o, y_o) = (0, 0)$ and $r_o = 5.5\text{m}$, and the length of the rod connecting the two MUs is fixed at $L = 22\text{m}$.

2.5.1 $x_{com}(0) = 30\text{m}$, $y_{com}(0) = 30\text{m}$, and $\phi(0) = \dot{x}_{com}(0) = \dot{y}_{com}(0) = \dot{\phi}(0) = 0$

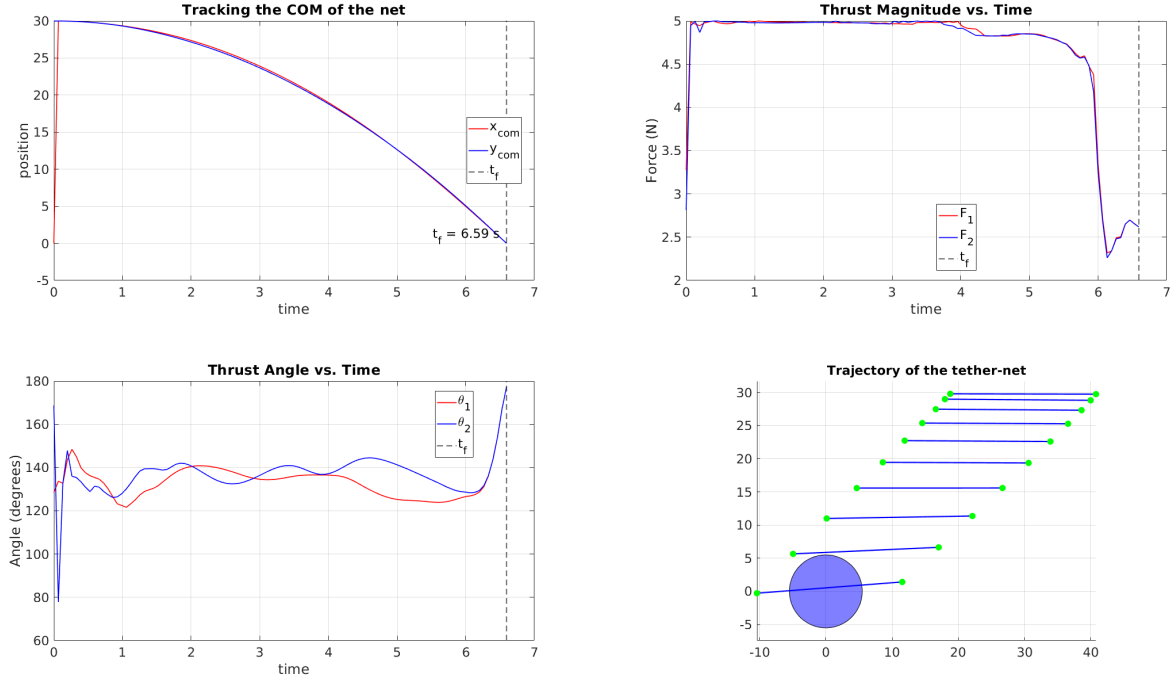


Figure 3: Results for the first set of initial conditions.

2.5.2 $x_{com}(0) = -30\text{m}$, $y_{com}(0) = 30\text{m}$, and $\phi(0) = \dot{x}_{com}(0) = \dot{y}_{com}(0) = \dot{\phi}(0) = 0$

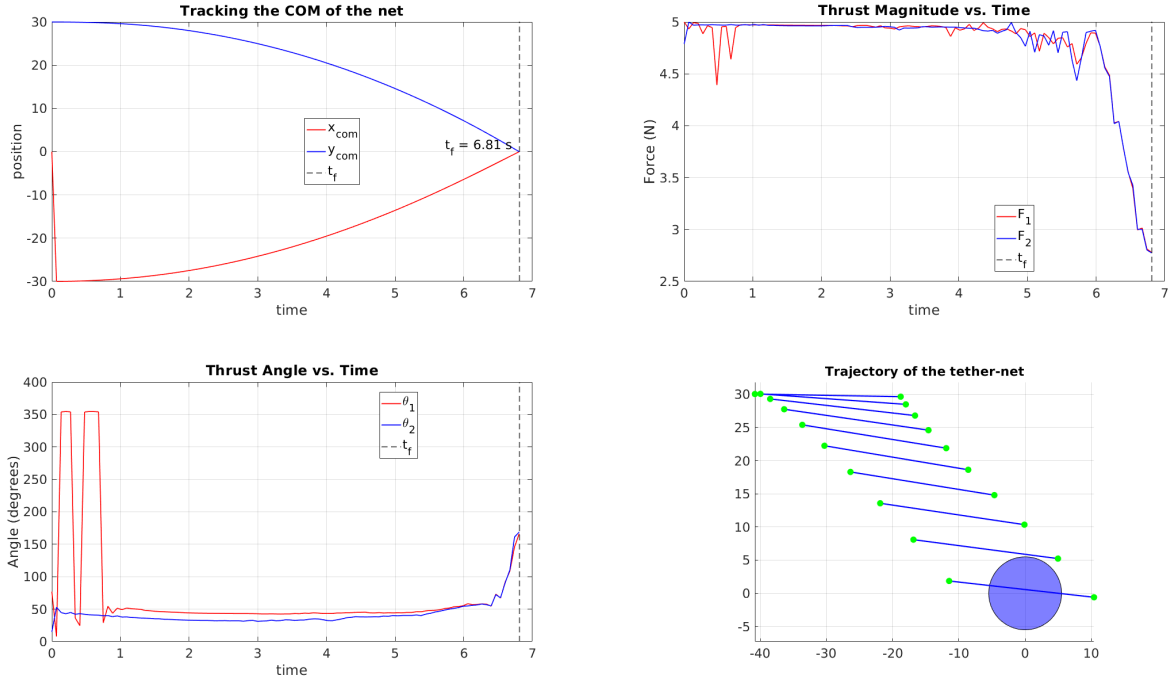


Figure 4: Results for the second set of initial conditions.

2.5.3 $x_{com}(0) = 30\text{m}$, $y_{com}(0) = 0\text{m}$, and $\phi(0) = \dot{x}_{com}(0) = \dot{y}_{com}(0) = \dot{\phi}(0) = 0$

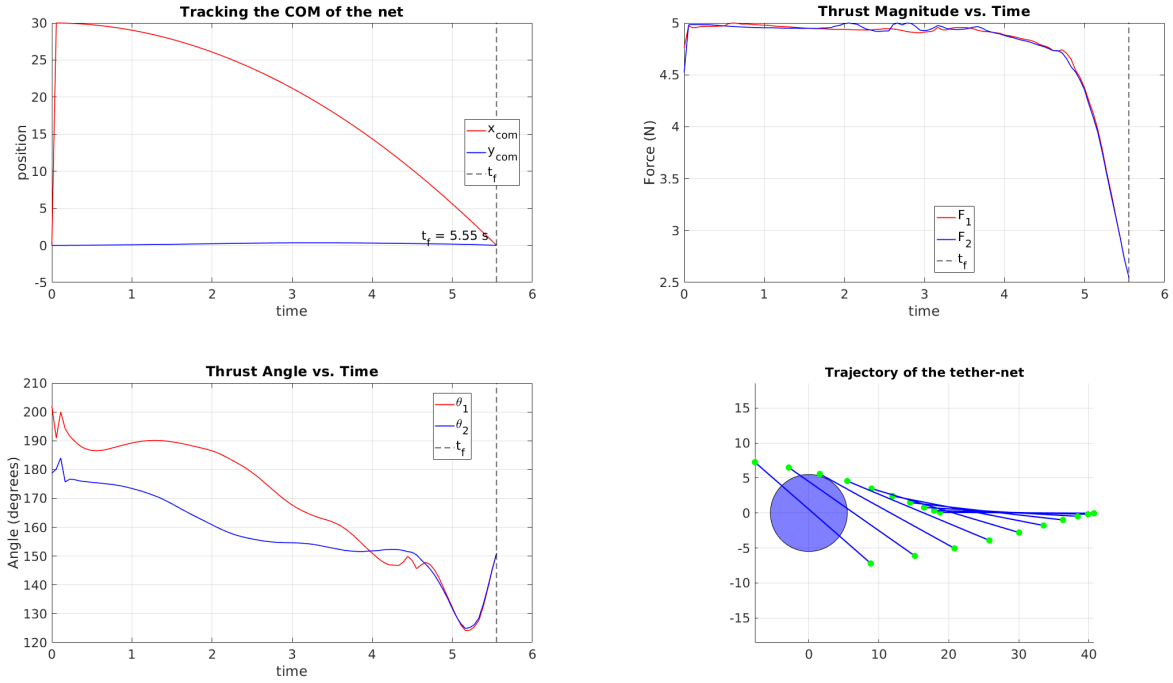


Figure 5: Results for the third set of initial conditions.

3 Case Study 2: Variable Mass and Flexible MUs Distance (Conducted by Feng Liu)

In this case study, the following changes are made in contrast to Section 2.

- The mass of the MUs will proportionally decrease over time based on the thrust magnitude.
- The distance between the MUs is no longer fixed and can vary between a predefined range.
- The MUs do not necessarily become stationary at the end of the mission.
- The initial positions of the MUs are different.
- All the variables are w.r.t the global coordinate frame for simplification.

In this section, and the following three subsections, the initial MU1 and MU2 positions are assumed to be at $[10, 10]m$ and $[32, 10]m$. The goal of the task is to maneuver the thrust magnitudes and angles of the two MUs so that their center position can reach the target's center of mass (CoM). The MUs should not enter the convex hull of the rotating target to avoid a collision, and the distance of the two MUs should maintain an interval to represent a not overly stretched but still wide-opening net mouth. The distance between the two MUs is 22 meters initially, and the distance can vary between 22 and 25 meters. The following assumptions are made to simplify the problem:

- The thrust magnitudes and angles can be changed instantaneously.
- The mass of the thread that connects the two MUs is negligible, so the thread is like a 'virtual rod' in the previous case study.
- No tension is generated from the thread between the two MUs, thus the dynamics of the two MUs are totally independent.

Three sub-case studies have been performed to explore the optimal control on the performance of the tether-net systems to minimize fuel consumption, time to complete the task, and both the time and fuel consumption.

3.1 Minimizing Fuel Consumption

In this research topic, the goal is to use optimal control to minimize fuel consumption when the MUs reach the closing condition. This objective can be further simplified into minimizing the integrated sum of the magnitude of the thrust during the task. In this part of the research, it is assumed that the total task time is fixed at 7 seconds. The value of this task time was picked arbitrarily based on test runs. The cost function is defined in Equation 9.

$$\min_{\mathbf{z}} J = \int_{t=0}^{t_f} (\mathbf{T}_1[t] + \mathbf{T}_2[t]) \Delta t \quad (9)$$

Where $\mathbf{z} = [\mathbf{x}_1, \mathbf{y}_1, \mathbf{x}_2, \mathbf{y}_2, \mathbf{T}_1, \mathbf{T}_2, \boldsymbol{\theta}_1, \boldsymbol{\theta}_2]$, the coordinates of MU1 and MU2 during the task are respectively defined by $\mathbf{x}_1, \mathbf{y}_1$ and $\mathbf{x}_2, \mathbf{y}_2$, the thrust magnitudes over time of the two MUs are defined by $\mathbf{T}_1, \mathbf{T}_2$ and the thrust angles are defined by $\boldsymbol{\theta}_1, \boldsymbol{\theta}_2$. To solve the problem with direct collocation, the time interval is divided into N time steps for discretization. The problem is then transformed into a nonlinear programming problem and the objective is modified to Equation 10.

$$\min_{\mathbf{z}} J = t_f \sum_{i=1}^N (\mathbf{T}_1[i] + \mathbf{T}_2[i]) \Delta t \quad (10)$$

in which the total number of time steps, N , is set to 50, and i represents the time step label, Δt is the duration of each time step.

The initial positions of the MUs are at $[10, 10]\text{m}$ and $[32, 10]\text{m}$, and they were stationary at that time. The mass of each MU is set to 2.5 kg at the beginning. Thus the following initial states are defined:

$$x_{1,t0} = 10, \quad y_{1,t0} = 10, \quad x_{2,t0} = 32, \quad y_{2,t0} = 10, \quad m_{1,t0} = 2.5, \quad m_{2,t0} = 2.5$$

The bounds of the variables in \mathbf{z} are set to:

$$\mathbf{x}[i], \mathbf{y}[i] \in [-20, 50]\text{m}, \quad \mathbf{T}[i] \in [5, 12]N, \quad \boldsymbol{\theta}[i] \in [0, 2\pi]\text{rad} \quad \forall i$$

The constraints of this nonlinear programming problem mainly from 5 aspects, and they are listed here:

- **Dynamics Constraints**

This set of constraints makes sure the states of the MUs follow the dynamics settings.

$$\mathbf{m}_1[i+1] = \mathbf{m}_1[i] - k\mathbf{T}_1[i]\Delta t, \quad \mathbf{m}_2[i+1] = \mathbf{m}_2[i] - k\mathbf{T}_2[i]\Delta t \quad (11)$$

Where i is the time step, k is the fuel consumption ratio which equals $0.0014 \text{ kg}/N \cdot \text{sec}^{-1}$.

$$\frac{d^2\mathbf{x}_1}{dt^2} = \frac{\mathbf{T}_1}{m_1} \cos(\boldsymbol{\theta}_1), \quad \frac{d^2\mathbf{y}_1}{dt^2} = \frac{\mathbf{T}_1}{m_1} \sin(\boldsymbol{\theta}_1), \quad \frac{d^2\mathbf{x}_2}{dt^2} = \frac{\mathbf{T}_2}{m_2} \cos(\boldsymbol{\theta}_2), \quad \frac{d^2\mathbf{y}_2}{dt^2} = \frac{\mathbf{T}_2}{m_2} \sin(\boldsymbol{\theta}_2) \quad (12)$$

$$\begin{aligned} \dot{\mathbf{x}}_1[i+1] &= \dot{\mathbf{x}}_1[i] + \frac{\mathbf{T}_1[i]}{\mathbf{m}_1[i]} \cos(\boldsymbol{\theta}_1[i])\Delta t, \\ \dot{\mathbf{y}}_1[i+1] &= \dot{\mathbf{y}}_1[i] + \frac{\mathbf{T}_1[i]}{\mathbf{m}_1[i]} \sin(\boldsymbol{\theta}_1[i])\Delta t \\ \dot{\mathbf{x}}_2[i+1] &= \dot{\mathbf{x}}_2[i] + \frac{\mathbf{T}_2[i]}{\mathbf{m}_2[i]} \cos(\boldsymbol{\theta}_2[i])\Delta t, \\ \dot{\mathbf{y}}_2[i+1] &= \dot{\mathbf{y}}_2[i] + \frac{\mathbf{T}_2[i]}{\mathbf{m}_2[i]} \sin(\boldsymbol{\theta}_2[i])\Delta t \end{aligned} \quad (13)$$

- **Final condition constraints**

This set of constraints controls the midpoint position between the two MUs at the end of the mission is at the target's CoM which is represented by $[x_o, y_o]$.

$$\frac{\mathbf{x}_1[t_f] + \mathbf{x}_2[t_f]}{2} = x_o, \quad \frac{\mathbf{y}_1[t_f] + \mathbf{y}_2[t_f]}{2} = y_o \quad (14)$$

- **MUs distance constraints**

This set of constraints maintains the net mouth (abstracted as the 'virtual rod') widely open in an acceptable range.

$$d_{\min} \leq \sqrt{(\mathbf{x}_2[i] - \mathbf{x}_1[i])^2 + (\mathbf{y}_2[i] - \mathbf{y}_1[i])^2} \leq d_{\max}, \quad \forall i \quad (15)$$

Where $d_{\min} = 22\text{m}$ and $d_{\max} = 25\text{m}$.

- **Total fuel consumption constraints**

In this case study, it is assumed that the fuel consumption should not exceed 0.5 kg, thus the mass of each MU at the end should not be below 2.0 kg. (This set of constraints was not implemented in the MATLAB code because it will never be violated.)

$$\mathbf{m}_1[i], \mathbf{m}_2[i] \geq 2.0, \quad \forall i \quad (16)$$

- Non-collision constraints

The MUs should not enter the convex hull of the rotating target, therefore:

$$\begin{aligned} (\mathbf{x}_1[i] - x_o)^2 + (\mathbf{y}_1[i] - y_o)^2 &\geq r_o^2, \quad \forall i, \\ (\mathbf{x}_2[i] - x_o)^2 + (\mathbf{y}_2[i] - y_o)^2 &\geq r_o^2, \quad \forall i, \end{aligned} \quad (17)$$

The initial guesses of the variables are set to:

$$\mathbf{x}_1 = \text{linspace}(x_{1,0}, x_o - 10, N)$$

$$\mathbf{x}_2 = \text{linspace}(x_{2,0}, x_o + 10, N)$$

$$\mathbf{y}_1 = \text{linspace}(y_{1,0}, y_o - 10, N)$$

$$\mathbf{y}_2 = \text{linspace}(y_{2,0}, y_o + 10, N)$$

$$\mathbf{T}_1, \mathbf{T}_2 = 6,$$

$$\boldsymbol{\theta}_1, \boldsymbol{\theta}_2 = 1.5\pi$$

3.2 Minimizing Mission Time

In this subsection's case study, we aim to minimize the total time for the MUs to reach the positions so that their midpoint is at the target's CoM. To handle the free endtime efficiently, the time horizon is normalized to a fixed interval between 0 and 1, so anywhere associated with t will be changed to $t = t_f \cdot \zeta$, where $\zeta \in [0, 1]$. For this subsection, the majority problem setup is the same as the one in Section 3.1, but with the following modifications:

- The final time, t_f , is added as a variable, so the variable set \mathbf{z} is now $[\mathbf{x}_1, \mathbf{y}_1, \mathbf{x}_2, \mathbf{y}_2, \mathbf{T}_1, \mathbf{T}_2, \boldsymbol{\theta}_1, \boldsymbol{\theta}_2, t_f]$, and the bounds of t_f is $[0.1, 20]$.
- The objective function is then changed to:

$$\min_{\mathbf{z}} J = t_f$$

- Add the initial guess of $t_f = 7$

Other than the above modifications, the problem setup of minimizing the time is the same as the setup of minimizing the fuel consumption.

3.3 Minimizing Both the Mission Time and Fuel Consumption

In this subsection, both the mission time and fuel consumption are minimized together. Because this is also a free-endtime problem, the time variable t is changed to $t = t_f \cdot \zeta$, where $\zeta \in [0, 1]$. The objective function is modified to:

$$\min_{\mathbf{z}} J = w_1 t_f + w_2 t_f \int_{\zeta=0}^1 (\mathbf{T}_1[\zeta] + \mathbf{T}_2[\zeta]) \Delta \zeta \quad (18)$$

Where w_1, w_2 are weight parameters for the objective of time and fuel. In this section, both of them are set to 1 so the two objectives are equally important.

To apply the collocation method, the objective function is discretized into:

$$\min_{\mathbf{z}} J = w_1 t_f + w_2 t_f \sum_{i=0}^N (\mathbf{T}_1[i] + \mathbf{T}_2[i]) \Delta t \quad (19)$$

The rest of the problem setup is the same as the Section 3.2.

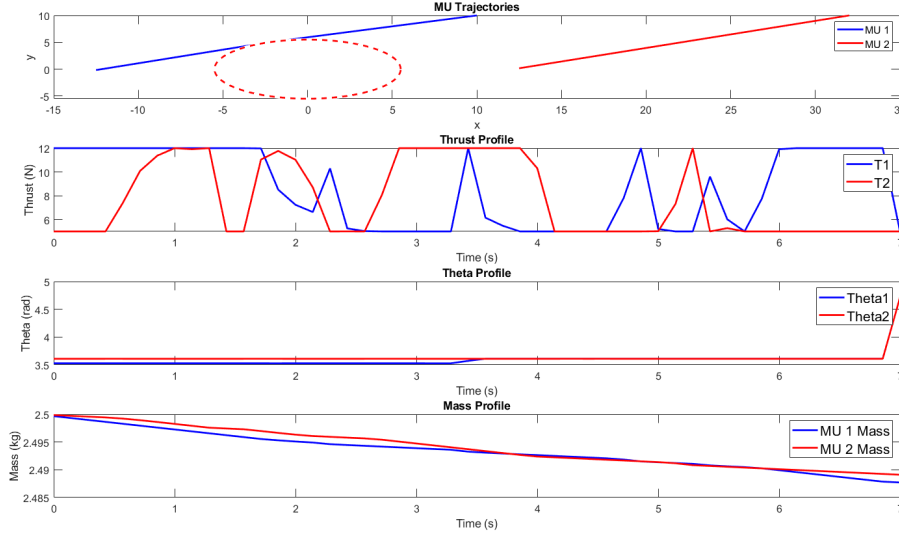


Figure 6: Result - Minimizing Fuel

3.4 Results

To solve the nonlinear programming problem, MATLAB `fmincon()` function is utilized. The option of running `fmincon()` was set to the default except 'MaxIterations' was increased to 1000. All three sub-case-studies were executed on a 16-core Processor Windows workstation with 64 GB RAM.

For the case study of minimizing the fuel consumption in 7 seconds, the optimization finished 1000 iterations in 67.5 seconds. The optimized fuel consumption is 0.1622 kg. Figure 6 shows the trajectories, thrust control profile, and the masses change over time.

For the case study of minimizing the mission time, the optimization converged at 238 iterations in 11.3 seconds. The optimized fuel consumption is 0.1633 kg, and the optimized mission time is 4.8384 seconds. Figure 7 shows the trajectories, thrust control profile and the masses change over time.

For the case study of minimizing both the mission time and the fuel consumption, the optimization converged at 88 iterations in 6.2 seconds. The optimized fuel consumption is 0.1630 kg, and the optimized mission time is 4.8487 seconds. Figure 8 shows the trajectories, thrust control profile, and the masses change over time.

Figure 9 shows the rendered results in the simulator created in Section 2.

References

- [1] T. J. Colvin, J. Karcz, and G. Wusk, "Cost and benefit analysis of orbital debris remediation," 2023.
- [2] B. Esmiller, C. Jacqueland, H.-A. Eckel, and E. Wnuk, "Space debris removal by ground- based lasers: main conclusions of the european project cleanspace," *Applied Optics*, vol. 53, no. 31, pp. I45–I54, 2014.
- [3] M. Shan, J. Guo, and E. Gill, "Review and comparison of active space debris capturing and removal methods," *Progress in Aerospace Sciences*, vol. 80, pp. 18–32, 2016.
- [4] Z. Meng, P. Huang, and J. Guo, "Approach modeling and control of an autonomous maneuverable space net," *IEEE Transactions on Aerospace and Electronic Systems*, vol. 53, no. 6, pp. 2651–2661, 2017.
- [5] P. Huang, D. Wang, Z. Meng, F. Zhang, and Z. Liu, "Impact dynamic modeling and adaptive target capturing control for tethered space robots with uncertainties," *IEEE/ASME Transactions on Mechatronics*, vol. 21, no. 5, pp. 2260–2271, 2016.

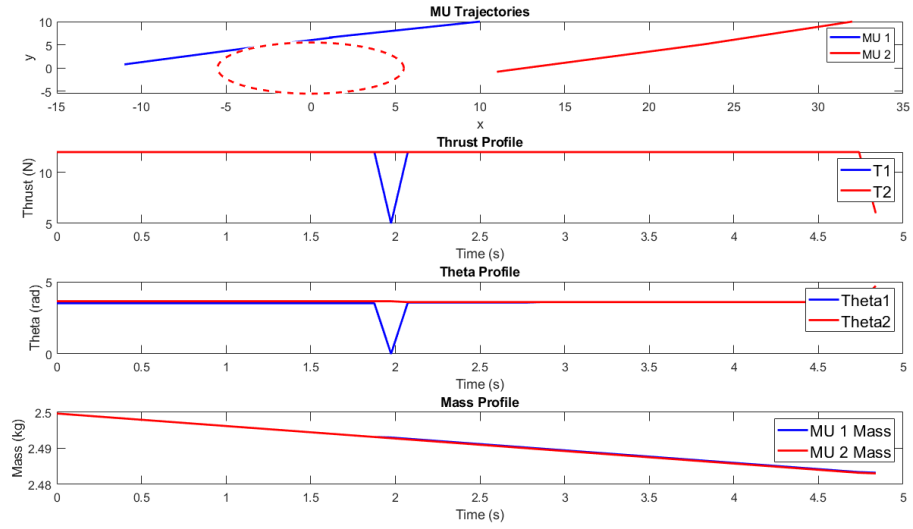


Figure 7: Result - Minimizing Time

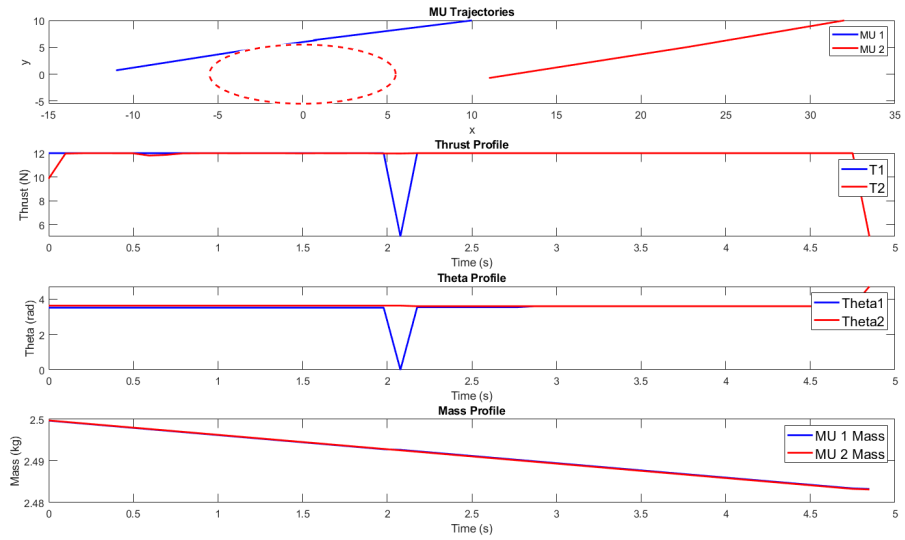
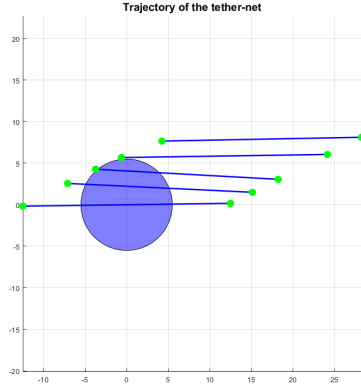
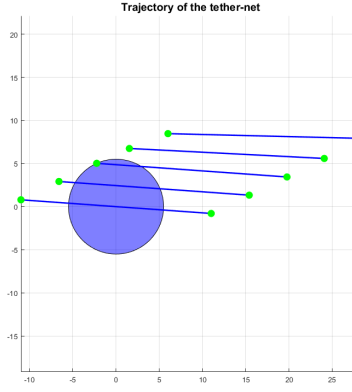


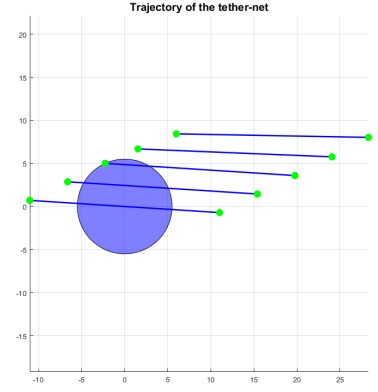
Figure 8: Result - Minimizing Both Time and Fuel



(a) Minimizing Fuel



(b) Minimizing Time



(c) Minimizing Time and Fuel

Figure 9: Case Study 2 - Rendered Trajectories

- [6] Y. Zhao, F. Zhang, P. Huang, and X. Liu, “Impulsive super-twisting sliding mode control for space debris capturing via tethered space net robot,” *IEEE transactions on industrial electronics (1982)*, vol. 67, no. 8, pp. 6874–6882, 2020.
- [7] F. Zhang and P. Huang, “Fuzzy-based adaptive super-twisting sliding-mode control for a maneuverable tethered space net robot,” *IEEE transactions on fuzzy systems*, vol. 29, no. 7, pp. 1739–1749, 2021.
- [8] A. Boonrath, F. Liu, E. M. Botta, and S. Chowdhury, “Learning-aided control of robotic tether-net with maneuverable nodes to capture large space debris,” *IEEE 2024 International Conference on Robotics and Automation*, 2024.
- [9] W. Zhu, Z. Pang, Z. Du, G. Gao, and Z. H. Zhu, “Multi-debris capture by tethered space net robot via redeployment and assembly,” *Journal of Guidance, Control, and Dynamics*, pp. 1–18, 2024.